RPS29 as a potential early diagnostic biomarker for necrotizing enterocolitis: validation from transcriptomic and proteomic cohorts

Zhe Wang[1,2#], Pengjian Zou[2#], Longlong Hou[2#], Jieting Lu[1], Jiahao Zeng[2], Pengfei Wei[2], Yu Ouyang[3], Yan Tian[4], Wei Zhong[2], Chaoting Lan[2], Huimin Xia[1,2], Kai Song[1]

[1]The First School of Clinical Medicine, Southern Medical University, Guangzhou, China; [2]Department of Pediatric Surgery, Guangzhou Women and Children's Medical Center, Guangzhou Medical University, Guangzhou, China; [3]Department of Pediatric Surgery, Guangzhou Women and Children's Medical Center, Liuzhou Hospital, Liuzhou, China; [4]Department of Anesthesiology, Jiangxi Provincial Children's Hospital, Nanchang Medical College, JXHC Key Laboratory of Jiangxi Provincial Children's Hospital, Nanchang, China

Contributions: (I) Conception and design: All authors; (II) Administrative support: W Zhong; (III) Provision of study materials or patients: Z Wang, P Zou, L Hou, W Zhong, C Lan; (IV) Collection and assembly of data: Z Wang, P Zou, L Hou, J Lu, J Zeng, P Wei, Y Ouyang, Y Tian; (V) Data analysis and interpretation: Z Wang, P Zou, C Lan, K Song; (VI) Manuscript writing: All authors; (VII) Final approval of manuscript: All authors.

[#]These authors contributed equally to this work.

Correspondence to: Chaoting Lan, PhD. Guangzhou Women and Children's Medical Center, Guangzhou Medical University, No. 9 Jinsui Road, Zhujiang New Town, Tianhe District, Guangzhou 510623, China. Email: 415879043@qq.com; Huimin Xia, PhD. The First School of Clinical Medicine, Southern Medical University, Guangzhou, China; Guangzhou Women and Children's Medical Center, Guangzhou Medical University, No. 9 Jinsui Road, Zhujiang New Town, Tianhe District, Guangzhou 510623, China. Email: huiminxia@hotmail.com; Kai Song, PhD. The First School of Clinical Medicine, Southern Medical University, No. 1838 Guangzhou Avenue North, Guangzhou 510515, China. Email: kaisonggz@163.com.

Background: Necrotizing enterocolitis (NEC) is a life-threatening gastrointestinal disorder in neonates, and its early diagnosis remains challenging. RPS29, a ribosomal protein associated with cellular stress and inflammation, was identified as significantly differentially expressed in the discovery proteomic screening. This study aimed to identify RPS29 as a potential biomarker for the early diagnosis of NEC.

Methods: In a prospective cohort, plasma samples were analyzed using Astral proteomics (controls, n=12; NEC stage I, n=12; NEC stage II, n=13; NEC stage III, n=12). Transcriptomic profiling was performed to assess mRNA expression in intestinal tissues from controls (n=5) and NEC patients (n=5). Plasma protein levels were further quantified by enzyme-linked immunosorbent assay (ELISA), while their expression in intestinal tissues from NEC infants and NEC mouse models was validated by immunofluorescence and reverse transcription-quantitative polymerase chain reaction (RT-qPCR). The diagnostic performance of plasma protein was evaluated using receiver operating characteristic (ROC) curves and compared with routine hematological parameters.

Results: RPS29 showed significantly decreased levels in the plasma of infants with NEC in the proteomic dataset, particularly in Bell stage I NEC. Plasma ELISA of RPS29 protein also revealed a significant decrease in RPS29 levels in Bell stage I NEC. RPS29 protein showed favorable diagnostic performance, with areas under the curve (AUCs) of 0.9679 and 0.9306 at stages II and III, and as high as 0.9861 at stage I. Intestine transcriptomics revealed a significant decrease of RPS29 in NEC patients, which was consistent with downregulation of RPS29 protein and mRNA expression validated in both NEC patients and mouse models.

Conclusions: Plasma RPS29 protein exhibits potential diagnostic accuracy for early-stage NEC and represents a promising biomarker for its early detection.

Keywords: Necrotizing enterocolitis (NEC); RPS29; inflammation; diagnostic biomarker; proteomic

Submitted Jan 20, 2026. Accepted for publication Apr 14, 2026. Published online May 26, 2026.
doi: 10.21037/tp-2026-1-0077
View this article at: https://dx.doi.org/10.21037/tp-2026-1-0077

Introduction

Necrotizing enterocolitis (NEC) is a severe acute gastrointestinal disease in preterm infants, characterized by high morbidity and mortality (1-3). Its pathogenesis is complex and progression is rapid, while the clinical manifestations are non-specific and often indistinguishable from other conditions, making early diagnosis particularly challenging (4,5). Without timely recognition and intervention, NEC can deteriorate rapidly and become life-threatening. Therefore, there is an urgent need to explore and identify reliable biomarkers to facilitate early and accurate diagnosis, advance understanding of disease mechanisms, and provide new strategies to improve neonatal outcomes.

However, currently used clinical markers, such as C-reactive protein (CRP) and lymphocyte, still lack sufficient sensitivity and specificity (6,7). In addition, several emerging biomarkers have also been investigated, including stool miR-223, the LIT score, circulating IL-1β, Gasdermin D, and IgG-tTG, but their reported diagnostic performance remains variable across studies (8-11). Recent advances in transcriptomic and proteomic profiling have facilitated the identification of novel biomarkers for early disease detection (12,13). However, the application of multi-omics approaches in identifying early diagnostic biomarkers for NEC remains limited. RPS29 encodes the 40S ribosomal protein S29. As an essential member of the ribosomal protein family, RPS29 participates in the maturation of 18S rRNA, the assembly of the 40S subunit, and the initiation of global protein translation. It also maintains the structural integrity of ribosomes in the cytoplasm, which is indispensable for fundamental cellular activities (14). Dysregulation of ribosomal proteins has been implicated in cellular stress responses and inflammation (15,16). In studies on preeclampsia, global gene expression profiling of cell-free RNA in amniotic fluid revealed a significant upregulation of RPS29, suggesting its potential as a novel biomarker (17). However, the role of RPS29 in NEC has not yet been reported.

This study, using plasma proteomic analysis, initially found that plasma RPS29 levels were significantly decreased in infants with NEC, particularly in NEC stage I. Plasma enzyme-linked immunosorbent assay (ELISA) further supported this finding. In addition, reduced plasma RPS29 showed good diagnostic performance for NEC stage I and was negatively correlated with inflammatory markers. Furthermore, in an NEC mouse model, intestinal transcriptomic analysis, together with validation in intestinal tissues from infants with NEC, showed that RPS29 expression was significantly decreased in the intestine. Taken together, we systematically evaluated the expression profile of RPS29 in NEC and indicated RPS29 may serve as a promising biomarker for the early diagnosis of NEC. We present this article in accordance with the ARRIVE reporting checklist (available at https://tp.amegroups.com/article/view/10.21037/tp-2026-1-0077/rc).

Highlight box

Key findings

- Plasma RPS29 levels were significantly decreased in neonates with necrotizing enterocolitis (NEC), particularly in Bell stage I NEC. RPS29 showed excellent early diagnostic performance, with an AUC of 0.9861 for stage I NEC. Consistent downregulation of RPS29 was further validated by enzyme-linked immunosorbent assay (ELISA), intestinal transcriptomic analysis, immunofluorescence, reverse transcription-quantitative polymerase chain reaction (RT-qPCR), and NEC mouse models.

What is known and what is new?

- NEC is a severe neonatal gastrointestinal disease with rapid progression, and its early diagnosis remains challenging. Conventional inflammatory markers, such as C-reactive protein (CRP), white blood cell (WBC) count, and lymphocyte count, have limited performance for early NEC detection.
- This study identifies RPS29 as a potential early diagnostic biomarker for NEC. Multi-omics analysis and experimental validation showed that RPS29 is decreased in both plasma and intestinal tissues of NEC patients, with supportive evidence from a neonatal NEC mouse model.

What is the implication, and what should change now?

- RPS29 may serve as a promising adjunctive biomarker for early NEC detection and may help improve timely clinical recognition. Larger multicenter studies and mechanistic investigations are needed before its routine clinical application.

Methods

Subjects

All samples used in this study were obtained from Guangzhou Women and Children's Medical Center. The study was conducted in accordance with the Declaration of Helsinki and its subsequent amendments. The study was approved by the Institutional Review Board of Guangzhou Women and Children's Medical Center (No. 2023307B01). Informed consent was obtained from the parents or legal guardians of all participants. The diagnosis of NEC was established according to the modified Bell's staging criteria

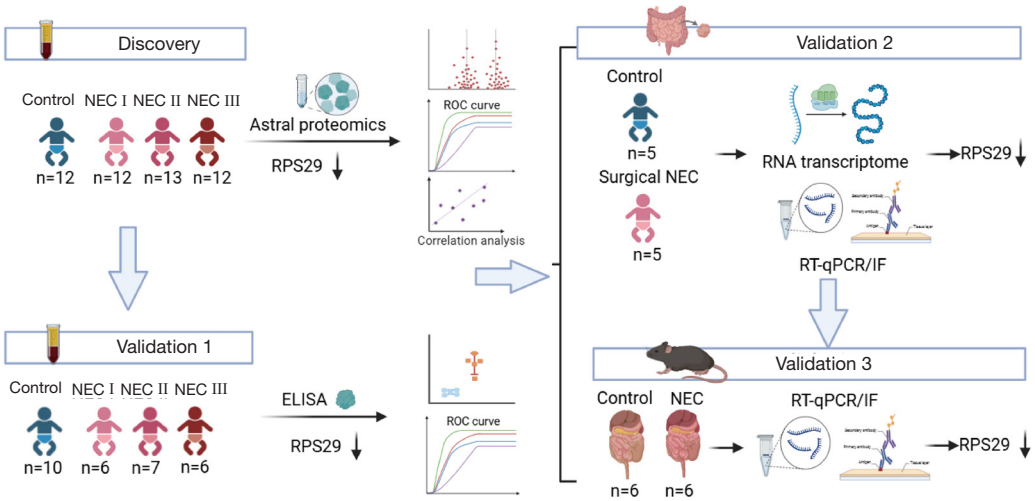

Figure 1 Study workflow for the identification and validation of RPS29 as a candidate diagnostic biomarker for NEC. In the discovery stage, plasma samples from control infants and infants with NEC were analyzed by Astral proteomics to identify differentially expressed proteins, and RPS29 was found to be decreased in NEC. In validation 1, plasma RPS29 levels were further measured by ELISA in an independent cohort, and its diagnostic performance was evaluated by ROC analysis. In validation 2, intestinal tissue samples from control and surgical NEC patients were analyzed using transcriptomic data and further validated by IF and RT-qPCR, which consistently showed decreased RPS29 expression in NEC. In validation 3, an NEC mouse model was used for additional verification, and RPS29 downregulation in intestinal tissues was confirmed by IF and RT-qPCR. ELISA, enzyme-linked immunosorbent assay; IF, immunofluorescence; NEC, necrotizing enterocolitis; ROC, receiver operating characteristic; RT-qPCR, reverse transcription-quantitative polymerase chain reaction.

(18), based on a comprehensive evaluation of systemic signs, intestinal signs, and radiologic features, and was confirmed during hospitalization by experienced neonatologists and pediatric surgeons. Infants with stage I NEC were diagnosed based on abdominal distension, gross bloody stool, and a positive fecal occult blood test, after exclusion of other intestinal diseases. Stage II NEC was defined as definite NEC, with additional findings such as decreased or absent bowel sounds and/or abdominal tenderness, together with radiologic evidence of intestinal dilatation, ileus, pneumatosis intestinalis, or portal venous gas. Stage III NEC was defined as advanced severe NEC developing on the basis of stage II disease, with manifestations including hypotension, bradycardia, severe apnea, combined respiratory and metabolic acidosis, generalized peritonitis, marked abdominal tenderness, abdominal distension, and radiologic evidence of ascites or pneumoperitoneum. For infants requiring surgery, the diagnosis was further supported by intraoperative findings and postoperative histopathological examination. A detailed study flowchart is presented in *Figure 1*. Neonates included in this study were diagnosed with NEC from 2022 to 2024 according to Bell's staging criteria, encompassing stages I–III. The control group consisted of neonates matched for gestational age and sex. To exclude interference from physiological abdominal distension, stage I NEC patients were required to meet the criteria of abdominal distension, positive fecal occult blood, and elevated infection markers. Exclusion criteria were (11,19): (I) severe congenital diseases; (II) family history of autoimmune disease; (III) incomplete clinical data; (IV) intestinal infectious diseases other than NEC. Ileal tissue specimens were divided into two groups: the NEC group (lesional ileal segments) and the control group (ileal tissues obtained from non-NEC neonates without intestinal inflammatory diseases, including intestinal obstruction and intestinal atresia, when conservative treatment was not feasible).

Basic demographic information (birth weight, gestational age and sex) and hematological parameters [CRP, neutrophil count, white blood cell (WBC) count, lymphocyte count] were obtained from the electronic medical records.

Plasma proteomics analysis

Astral proteomics was employed to analyze samples from controls (n=12) and pediatric patients with NEC at stage I

Table 1 The cohort of basic characteristics of NEC and control

Characteristics	Control	NEC
Number of patients	12	37
Gender (female/male)	3/9	12/25
Gestational age at birth (weeks)	31 (29.25–34.75)	31 (29.5–36)
Birth weight (kg)	1.64 (1.19–2.14)	1.61 (1.13–2.34)
Postnatal blood sampling time (days)	1 (1–7.15)	13 (7.5–21.5)

Data are presented as number or median (interquartile range). NEC, necrotizing enterocolitis.

(n=12), stage II (n=13), and stage III (n=12) (*Table 1*). Plasma samples (5 µL) were denatured in 50 µL of buffer containing 8 M urea in 100 mM ammonium bicarbonate. Proteins were reduced with 10 mM DTT at 37 ℃ for 30 min and subsequently alkylated with 50 mM IAA in the dark at room temperature. The samples were then diluted with 50 mM ammonium bicarbonate and digested with trypsin (Promega, Madison, WI, USA) at a 50:1 substrate-to-enzyme ratio overnight at 37 ℃. Resulting peptides were desalted using C18 StageTips (Thermo Fisher Scientific, Rockford, IL, USA) prior to LC-MS analysis, and their concentrations were determined by OD280 measurement on a NanoDrop One spectrophotometer (Thermo Fisher Scientific, Waltham, MA, USA). Data-independent acquisition (DIA) mode was applied with optimized parameters provided by the manufacturer. DIA raw files were processed using DIA-NN (v1.8.1). Spectra were searched against the UniProtKB/Swiss-Prot human protein database with trypsin specificity. Carbamidomethylation of cysteine was set as a fixed modification, and oxidation of methionine and N-terminal acetylation as variable modifications. The false discovery rate (FDR) was controlled below 1% at peptide and protein levels. The omics dataset was used as an exploratory screening tool rather than for comprehensive system level characterization of all differentially expressed molecules.

ELISA

We used RPS29 ELISA kit from Zhenke Bio (Shanghai, China; Cat. No. ZK-15737) to detect the levels of RPS29 protein and its autoantibodies in the plasma of the control, stage I NEC, stage II NEC and stage III NEC groups. The ELISA procedure was conducted according to the manufacturer's instructions.

Mouse experiments

All animal procedures were approved by the Animal Ethics Committee of Guangdong Huawei Testing Co., Ltd. (No. 202509001), in accordance with institutional and national guidelines for the care and use of laboratory animals. Neonatal C57BL/6 mice were obtained from the Guangdong Provincial Experimental Animal Center (Production License No. SCXK (Yue) 2022-0002) and maintained under specific pathogen-free (SPF) conditions. Animals were housed in a barrier facility with strictly controlled temperature, humidity, and light-dark cycles, and neonatal mice were kept in a thermostatically controlled incubator to ensure stable body temperature and minimize environmental stress. All animals had access to appropriate nutrition and water and were monitored daily for health status. For tissue and blood sample collection, procedures were performed by trained personnel following standardized operating protocols, and anesthesia with isoflurane was applied during terminal procedures to minimize pain and distress. Humane endpoint criteria were predefined, including persistent inability to feed, severe lethargy, respiratory distress, hypothermia, or moribund state; animals meeting these criteria were immediately euthanized. At experimental endpoints, animals were humanely euthanized by overdose of anesthetics, and carcasses were sealed, stored at –20 ℃, and disposed of by a licensed professional company through harmless biological waste treatment. The NEC mouse model was established as previously described (20,21). Briefly, 4-day-old C57BL/6 mice were orally gavaged with adult mouse cecum-derived bacteria (3.5×10^7 CFU/mouse). Starting the next day, mice were subjected to hypoxia-cold shock cycles (twice daily) and formula feeding four times daily (40 µL per feed) for

Table 2 Primer sequence list for RT-qPCR

Primer name	Forward sequence (5'→3')	Reverse sequence (5'→3')	Species
RPS29	CGCTCTTGTCGTGTCTGTTCA	CCTTCGCGTACTGACGGAAA	Human
Rps29	GTCTGATCCGCAAATACGGG	AGCCTATGTCCTTCGCGTACT	Mouse
GAPDH	CTGGGCTACACTGAGCACC	AAGTGGTCGTTGAGGGCAATG	Human
Gapdh	AGGTCGGTGTGAACGGATTTG	TGTAGACCATGTAGTTGAGGTCA	Mouse

RT-qPCR, reverse transcription-quantitative polymerase chain reaction.

4 days. Each hypoxia-cold shock cycle consisted of exposure to 5% O_2 for 2 min, followed by cold stimulation at 4 ℃ for 10 min. Breastfed control mice remained with their dams until euthanasia. Mice were induced with 4% isoflurane in a prefilled chamber (O_2 1.0 L/min) until loss of righting reflex (approximately 2 min), then maintained at 2% via nose cone. After confirming a surgical plane of anesthesia (absence of pedal and corneal reflexes) for ≥5 min, cervical dislocation was performed. Small intestines were examined macroscopically and fixed in buffered formalin for hematoxylin and eosin (H&E) staining. Small intestines were placed in buffered formalin for H&E staining to estimate the H&E scores graded 0–4 (22). The H&E scores of 2–4 are defined as the occurrence of NEC.

Transcriptomics analysis

Total RNA was extracted from 30–50 mg snap-frozen intestinal tissues from NEC and control neonates using TRIzol™ reagent (Invitrogen, Carlsbad, CA, USA) according to the manufacturer's instructions. RNA concentration, purity and integrity were then further assessed. Libraries were prepared from 1 μg of total RNA per sample using the NEBNext® Ultra™ II RNA Library Prep Kit for Illumina (New England Biolabs, Ipswich, MA, USA), incorporating poly(A) mRNA enrichment. Paired-end sequencing (150 bp) was performed on an Illumina NovaSeq™ 6000 platform (Illumina, San Diego, CA, USA), generating ~40 million paired-end reads per sample. Raw sequencing data quality was assessed with FastQC (v0.12.1) and trimmed using TrimGalore. The transcriptomic dataset was used to validate the candidate findings from the proteomic screening, rather than to analyze the entire set of transcriptomic data.

Identification of differentially expressed genes

Differential expression analysis of the transcriptomic data was performed on the raw count matrix using DESeq2 in R (version 4.2.1) following the standard workflow. Raw count data were further transformed using the variance stabilizing transformation (VST) method implemented in DESeq2 to generate normalized expression values for visualization.

Reverse transcription-quantitative polymerase chain reaction (RT-qPCR)

Total RNA was extracted from intestinal tissue using TRIzol reagent (Invitrogen). Reverse transcription was performed with 1 μg of total RNA using the HiScript III RT SuperMix for qPCR (+gDNA wiper) kit (Vazyme, Nanjing, China; R323-01). The reaction conditions were as follows: 42 ℃ for 2 minutes, followed by the addition of 4 μL of 5X HiScript III RT SuperMix and incubation at 37 ℃ for 10 minutes, with a final step at 85 ℃ for 5 seconds. Quantitative PCR (qPCR) was carried out using Vazyme's Universal SYBR qPCR Master Mix on a Thermo Real-Time qPCR instrument. The relative mRNA expression levels of target genes were calculated using the $2^{-\Delta\Delta CT}$ method. Primer sequences are detailed in *Table 2*.

Immunofluorescence staining

Paraffin-embedded tissue sections were deparaffinized, rehydrated and subjected to antigen retrieval using EDTA or citric acid buffer. After permeabilization with 0.1% Triton X-100 (20 min, RT), sections were washed three times with PBS. Non-specific binding was blocked with 20% goat serum (1 h, RT), followed by overnight incubation with primary antibodies at 4 ℃. After PBS washes, sections were incubated with Goat Anti-Rabbit IgG (1:500, E032220-01, Earthox, Burlingame, CA, USA; 1 h, RT), washed again, and counterstained with DAPI (G1401, Servicebio, Wuhan, China). Imaging was performed using a fluorescence microscope (Leica Microsystems, Wetzlar, Germany). Primary antibodies used: RPS29 (1:300 dilution, 17374-1-

AP, Proteintech, Rosemont, IL, USA).

H&E staining

Ileal tissue samples were collected from NEC patients during surgical treatment and from ileal tissue samples from non-NEC infants. They were fixed with 4% paraformaldehyde. After standard dehydration procedures, colonic tissues were embedded in wax blocks and cut into 4 µm sections. Normal intestinal tissue and NEC lesion intestinal sections were stained with H&E.

Statistical analysis

All data are presented as mean ± standard error of the mean (SEM). Statistical analyses were performed using GraphPad Prism (version 10.2). For comparisons between two groups, an unpaired Student's t-test was used. Spearman's rank correlation coefficient was used to evaluate correlations between variables. Receiver operating characteristic (ROC) curves were generated to assess diagnostic performance, and the area under the curve (AUC) was calculated. The optimal cutoff value was determined using the maximum Youden index, and the corresponding sensitivity and specificity were reported. $P<0.05$ was considered statistically significant.

Results

Characteristics of the subject

A total of 37 neonates with NEC (NEC I = 12, NEC II =13, NEC III = 12) and 12 neonates without NEC were recruited based on predefined inclusion and exclusion criteria, the cohort of basic characteristics of NEC and control in *Table 1*. Surgical intestinal tissue samples were obtained from 5 NEC patients and 5 non-NEC patients. The study flowchart is illustrated in *Figure 1*.

RPS29 is significantly down-regulated in the plasma of NEC group, with preliminary evidence of early diagnostic relevance

Astral proteomics analysis of peripheral blood revealed a significant reduction of RPS29 in the plasma of NEC patients, spanning all disease stages (I–III), with corresponding P values of <0.0001, <0.0001, and 0.0001, respectively (*Figure 2A*). ROC curve analysis further suggested that RPS29 exhibited promising diagnostic performance across all stages of NEC, with AUC values of 0.9679 (sensitivity =92.31%, specificity =91.67%) and 0.9306 (sensitivity =83.33%, specificity =91.67%) in stage II and stage III patients, respectively. Notably, in stage I NEC patients, RPS29 maintained favorable early diagnostic capability, with an AUC as high as 0.9861 (sensitivity =100%, specificity =91.67%) (*Figure 2B*). We analyzed commonly used clinical inflammatory markers in the enrolled subjects (control group and NEC stages I–III) who had undergone peripheral blood proteomic profiling. The results showed that the WBC counts did not exhibit significant statistical differences across the NEC stages (Figure S1A,S1B). CRP was significantly elevated in NEC stage II and stage III, with P values of 0.01 and <0.0001 (Figure S1C), respectively, and corresponding AUC values of 0.7885 and 1.0 (Figure S1D). Lymphocyte counts were also significantly decreased in NEC stage II and stage III, with P values of 0.009 and 0.0003 (Figure S1E), and corresponding AUC values of 0.8013 and 0.9097 (Figure S1F). Notably, in NEC stage I, neither CRP nor lymphocyte counts showed significant differences compared with the control group.

We validated RPS29 protein levels using ELISA in an independent NEC cohort. The results were largely consistent with the proteomic analysis, showing significant downregulation of RPS29 in NEC patients, with corresponding P values of <0.0001, 0.0009, and 0.007 for stages I–III, respectively (*Figure 2C*). Further ROC curve analysis revealed AUC values of 1.0 (sensitivity =100%, specificity =100%), 0.9286 (sensitivity =85.71%, specificity =90%), and 0.8667 (sensitivity =83.33%, specificity =90%) for stages I, II, and III, respectively (*Figure 2D*).

RPS29 is significantly downregulated in the intestines of NEC patients

By collecting intestinal tissues from surgically treated infants, we observed that NEC patients exhibited marked intestinal edema and necrosis during surgery (*Figure 3A*), and H&E staining revealed disruption of the intestinal mucosal structure along with inflammatory cell infiltration (*Figure 3B*). Further transcriptomic analysis of the intestinal tissues showed a significant downregulation of RPS29 in the NEC group (P=0.004) (*Figure 3C*). Validation by quantitative RT-qPCR also showed reduced RPS29 expression (P=0.008) (*Figure 3D*). In addition, immunofluorescence staining of RPS29 protein levels suggested a significant decrease in NEC intestinal tissues,

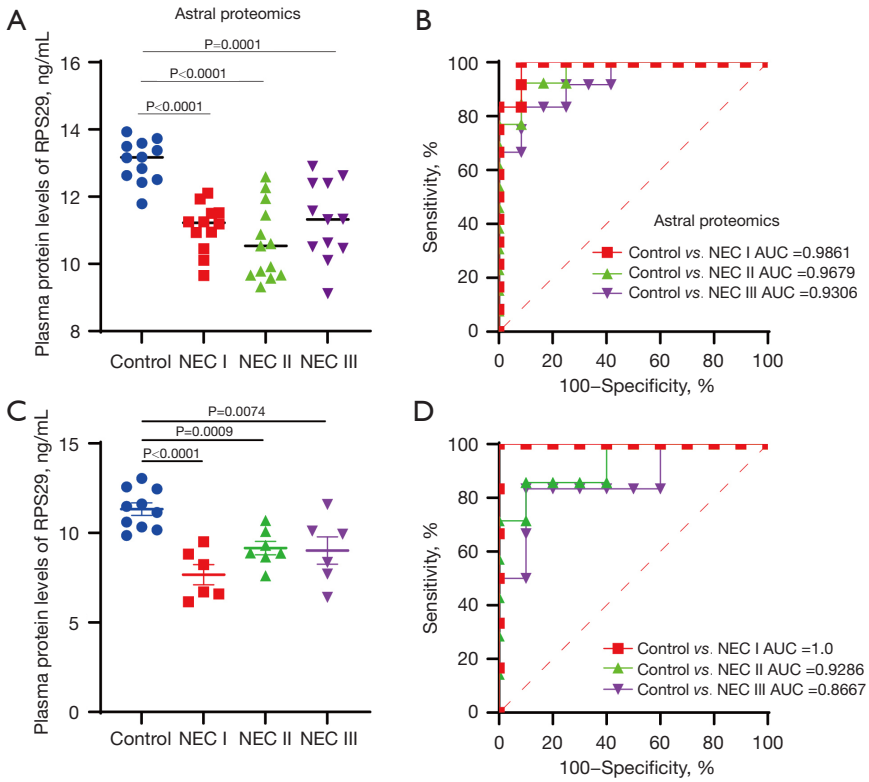

Figure 2 Expression of RPS29 in NEC plasma sequencing. (A) Plasma protein levels of RPS29 across control, NEC I, NEC II, and NEC III groups measured by Astral proteomics. (B) ROC curves evaluating the diagnostic performance of plasma RPS29 levels measured by Astral proteomics for differentiating NEC I, NEC II, and NEC III from controls. (C) Plasma RPS29 protein levels were quantified using ELISA. (D) ROC curves evaluating the diagnostic performance of plasma RPS29 levels measured by ELISA for differentiating NEC I, NEC II, and NEC III from controls. Each point represents an individual patient, and the line represents the mean ± SEM. P values were determined using unpaired t-test (two-tailed). AUC, area under the curve; ELISA, enzyme-linked immunosorbent assay; NEC, necrotizing enterocolitis; ROC, receiver operating characteristic; SEM, standard error of the mean.

with quantitative fluorescence analysis yielding a P value of 0.03 (*Figure 3E,3F*).

RPS29 expression was decreased in the intestinal tissues of NEC mice

We further examined the expression of RPS29 in the intestinal tissues of NEC mouse models (*Figure 4A*). Compared with control mice, NEC mice exhibited impaired growth and development (*Figure 4B*), and their intestines showed signs of distension and edema (*Figure 4C*). H&E staining revealed sparse intestinal villi, pronounced epithelial cell shedding, and thinning of the intestinal wall (*Figure 4D*), confirming the successful establishment of the model. Immunofluorescence staining suggested a significant reduction of RPS29 expression in the intestinal tissues of NEC mice, with quantitative fluorescence analysis yielding a P value of 0.002 (*Figure 4E,4F*). RT-qPCR further supported the downregulation of RPS29 mRNA, with a P value of 0.01 (*Figure 4G*).

The correlation between plasma RPS29 content and blood routine indicators in NEC

Given that inflammatory markers such as CRP, WBC count, neutrophil count, and lymphocyte count are commonly used in the clinical evaluation of NEC and are associated with disease activity and progression (6,7,23,24), with neutrophils and lymphocytes also implicated in mechanistic studies of NEC pathogenesis (25,26), we further assessed whether plasma RPS29 levels were correlated with these indicators in NEC patients. To further investigate the role of RPS29 in

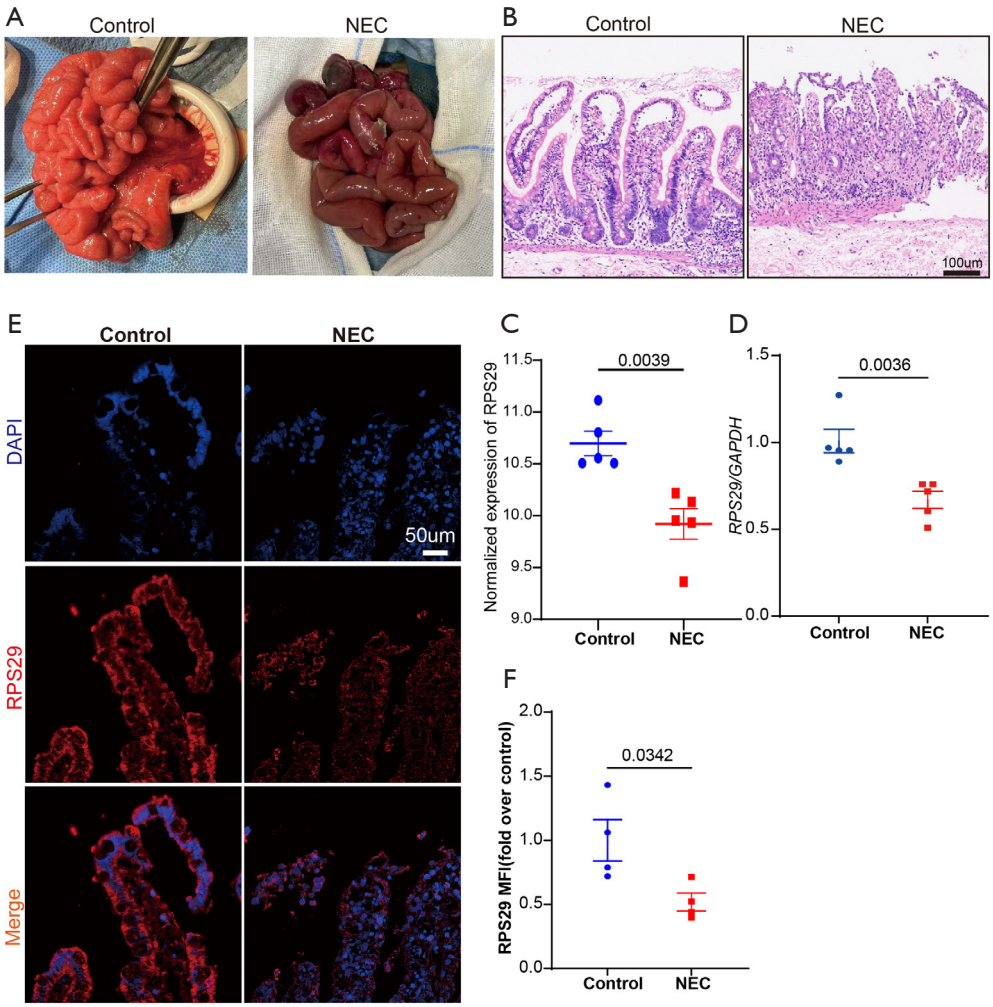

Figure 3 RPS29 levels in intestinal tissues of neonates with NEC. (A) Intraoperative control and intestinal tissues from neonate with NEC. (B) Representative hematoxylin and eosin staining of intestinal tissues in NEC compared with controls. (C) Intestinal transcription levels of RPS29 in the NEC and control groups determined by transcriptome sequencing. (D) Relative mRNA expression of RPS29 in intestinal tissues determined by RT-qPCR in NEC compared with controls. (E) Representative immunofluorescence staining of RPS29 (red) of intestine in NEC compared with controls. (F) Quantification of RPS29 immunofluorescence intensity in NEC compared with controls. Each point represents an individual patient, and the line represents the mean ± SEM. P values were determined using unpaired t-test (two-tailed). NEC, necrotizing enterocolitis; RT-qPCR, reverse transcription-quantitative polymerase chain reaction; SEM, standard error of the mean.

the clinical progression of NEC, we identified a correlation between plasma RPS29 content and inflammatory indicators in the complete blood count of NEC (*Figure 5*). Plasma RPS29 protein levels were negatively correlated with inflammatory markers in the complete blood count of NEC patients, including CRP (r=–0.5540, P=0.002), WBC (r=–0.3903, P=0.03), neutrophils (r=–0.4614, P=0.008) and lymphocytes (r=–0.3633, P=0.049).

Discussion

NEC is an acute inflammatory gastrointestinal disease that can rapidly progress to intestinal necrosis, posing a serious threat to neonatal survival. Early diagnosis is critical for timely intervention and improved outcomes. In this study, intestinal RNA transcriptome sequencing and peripheral plasma proteomics revealed that RPS29 was altered at the

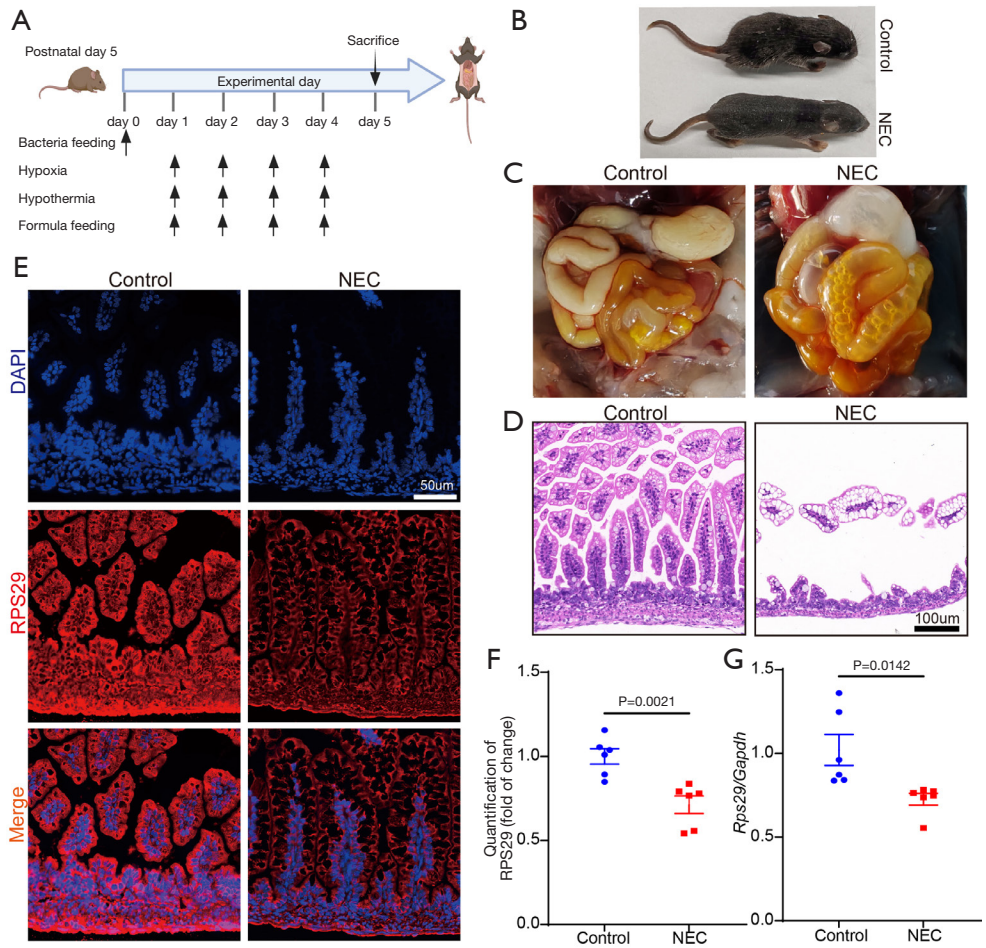

Figure 4 RPS29 levels in intestinal tissues of control mice with NEC. (A) Schematic diagram of NEC mouse modeling. (B) Appearance of control and NEC-induced mice. (C) Gross morphology of mouse intestines in NEC compared with controls. (D) Representative hematoxylin and eosin staining of intestinal tissues in NEC compared with controls. (E) Representative immunofluorescence staining of RPS29 (red) in intestine of NEC compared with controls. (F) Quantification of RPS29 immunofluorescence intensity, demonstrating significantly lower levels in NEC mice compared with controls. (G) Relative mRNA expression of RPS29 in intestinal tissues determined by RT-qPCR in NEC compared with controls. Each point represents an individual mouse, and the line represents the mean ± SEM. P values were determined using unpaired t-test (two-tailed). NEC, necrotizing enterocolitis; RT-qPCR, reverse transcription-quantitative polymerase chain reaction; SEM, standard error of the mean.

early onset of NEC and exhibited favorable diagnostic performance. Subsequent validation in a NEC mouse model and intestinal tissues from NEC infants supported the decreased expression of RPS29. Correlation analysis with clinical indicators further showed that decreased RPS29 levels were associated with elevated inflammatory markers. These findings suggest that RPS29 may serve as a promising biomarker for the early diagnosis of NEC. In addition, the changes observed in the animal model were consistent with those seen in clinical disease, providing a basis for further mechanistic investigation of RPS29.

Early diagnosis is a critical step in the clinical management of NEC. Conventional indicators such as CRP, WBC, platelet count (PLT), and IL-6 are primarily used for the differential diagnosis of surgical NEC (27-30), as they typically increase only after intestinal necrosis or perforation, leading to a delayed diagnostic window. In our study, RPS29 not only exhibited promising early diagnostic capability in NEC I but also maintained high diagnostic accuracy in NEC II, suggesting potential predictive

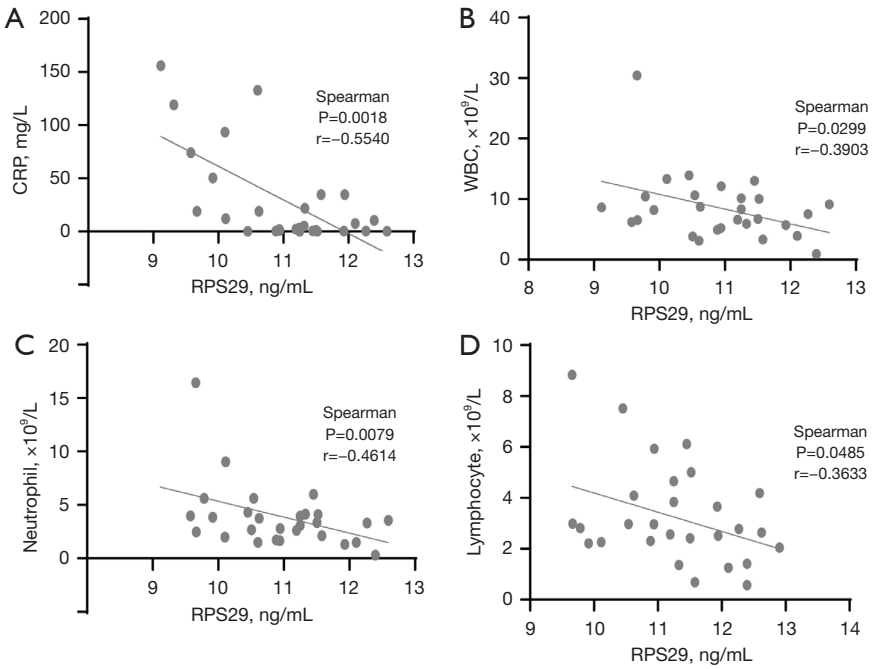

Figure 5 Plasma RPS29 in NEC patients is correlated with inflammatory indicators in the complete blood count. Spearman correlation analysis was performed between plasma RPS29 expression levels and (A) CRP, (B) WBC, (C) neutrophil count, and (D) lymphocyte count. CRP, C-reactive protein; NEC, necrotizing enterocolitis; WBC, white blood cell.

value for disease progression. In terms of sensitivity and specificity, previous studies have shown that several reported biomarkers for NEC exhibit variable diagnostic performance. Fecal calprotectin and miR-223 have been reported with a sensitivity of 75% and a specificity of 62% (31), whereas plasma Gasdermin D showed a sensitivity of 77% but a relatively low specificity of 22% (10). Similarly, IL-6 and IL-33 exhibited high sensitivity (100%) but only moderate specificity (30). In stage I NEC, our results showed that RPS29 could achieve an AUC of 0.9861, with a sensitivity of 100% and a specificity of 91.67%, indicating strong early diagnostic performance. Furthermore, RPS29 maintained diagnostic performance in stage II and stage III NEC, with sensitivities of 92.31% and 83.33%, respectively, while specificity remained stable at 91.67%. The identification of RPS29 complements our previous findings on early diagnostic markers IgG tTG (11) and AQP-4 (19), and shows superior early diagnostic performance compared to AQP-4 and IgG tTG.

The ribosome is the core machinery for protein translation and plays a critical role in maintaining protein homeostasis. As a key regulator of cellular growth, proliferation, and metabolic activities, the proteins synthesized by ribosomes constitute almost all fundamental components of living organisms. Ribosomal dysfunction has been implicated in aberrant protein synthesis and is closely associated with the development and progression of various intestinal diseases (32). Previous studies have indicated that ribosome-associated proteins play important roles in intestinal diseases and tumors. For example, frameshift mutations in RPL22 are associated with colorectal cancer, while RPL23A regulates the cell cycle and proliferation and is considered a potential therapeutic target and prognostic biomarker (33,34). The translation factor eIF5A has been shown to exert pro-inflammatory effects during inflammation (35), and impaired ribosome biogenesis has also been observed in animal models of inflammatory bowel disease (36). Although studies on RPS29 in intestinal diseases remain limited, existing evidence suggests that it is closely linked to immune regulation and tissue homeostasis. RPS29 can regulate inflammation and apoptosis through alternative splicing regulatory networks and is positively associated with tumor immune cell infiltration (37,38). In high-altitude cerebral edema (HACE), dysregulation of RPS29 is closely related to ribosomal stress, disrupted oxidative phosphorylation, and impaired cell survival pathways (39,40). Mechanistic studies have shown that RPS29 deficiency activates the p53 signaling pathway, thereby inducing pro-inflammatory cytokine expression

and forming a "ribosomal stress-inflammation" feedback loop (16). In the present study, we found that RPS29 expression was significantly downregulated in both NEC infants and NEC mouse models. Early ribosomal dysfunction may lead to defective protein synthesis, impair the reparative capacity of the intestinal epithelial barrier, and disrupt immune homeostasis, thereby exacerbating intestinal necrosis and inflammatory injury. These findings suggest that RPS29 may play an important role in the pathogenesis of NEC and provide a potential target for future mechanistic studies and therapeutic interventions.

Several limitations of this study should be noted. First, the present study has a relatively limited sample size and population diversity. Therefore, multicenter studies with larger and more heterogeneous cohorts are needed to further confirm the robustness and generalizability of RPS29 before it can be applied in clinical practice. Second, all participants were recruited from southern China, and potential influences of demographic factors such as region, ethnicity, sex, and birth weight were not fully considered. Additionally, although this study suggests the potential value of RPS29 for early diagnosis of NEC, its specific role in the pathogenesis of NEC remains insufficiently elucidated. In addition, there was a certain difference in sampling time between the control and NEC groups, which may have affected RPS29 levels. Moreover, although abdominal distension is common in preterm infants, it was not analyzed separately in the present study and therefore still warrants further investigation. Moreover, a sepsis control cohort was not included in the present study, which limited our ability to further assess the specificity of RPS29 for NEC, particularly in distinguishing NEC from neonatal sepsis and other systemic inflammatory conditions. Future studies should incorporate such disease controls to strengthen the evaluation of its specificity and differential diagnostic value. Furthermore, animal models or organoid systems, combined with multi-omics approaches, could be employed to further investigate the functional mechanisms of RPS29 in intestinal inflammation and immune regulation, and to evaluate its feasibility as a potential therapeutic target.

Conclusions

In conclusion, our results suggest that RPS29 has significant diagnostic value for NEC and may serve as a biomarker for its early detection. Given its association with immunity, oxidative stress, and apoptosis, further investigation into the role of RPS29 in NEC pathogenesis may reveal novel strategies for prevention and treatment in neonates.

Acknowledgments

We would like to thank the Clinical Biological Resource Bank of Guangzhou Women and Children's Medical Center for providing the clinical samples.

Footnote

Reporting Checklist: The authors have completed the ARRIVE reporting checklist. Available at https://tp.amegroups.com/article/view/10.21037/tp-2026-1-0077/rc

Data Sharing Statement: Available at https://tp.amegroups.com/article/view/10.21037/tp-2026-1-0077/dss

Peer Review File: Available at https://tp.amegroups.com/article/view/10.21037/tp-2026-1-0077/prf

Funding: This study was supported by grants from the Science and Technology Project of Guangzhou (Nos. 20261A031036, 2024A03J1238, 2024A03J1171 and 2025A03J4456), the National Natural Science Foundation of China (Nos. 82301955, 82370526 and 82460317), the Guangdong Basic and Applied Basic Research Foundation (No. 2024A1515013190), the Guangzhou Major Difficult and Rare Diseases Project (No. 2024MDRD17) and the Basic and Applied Basic Research Foundation of Guangxi Province of China (No. 2024JJB140724).

Conflicts of Interest: All authors have completed the ICMJE uniform disclosure form (available at https://tp.amegroups.com/article/view/10.21037/tp-2026-1-0077/coif). H.X. serves as an unpaid editorial board member of *Translational Pediatrics* from July 2025 to June 2026. The other authors have no conflicts of interest to declare.

Ethical Statement: The authors are accountable for all aspects of the work in ensuring that questions related to the accuracy or integrity of any part of the work are appropriately investigated and resolved. The study was conducted in accordance with the Declaration of Helsinki and its subsequent amendments. The study was approved by the Institutional Review Board of Guangzhou Women and Children's Medical Center (No. 2023307B01). Informed consent was obtained from the parents or legal guardians of all participants. All animal procedures were approved

by the Animal Ethics Committee of Guangdong Huawei Testing Co., Ltd. (No. 202509001), in accordance with institutional and national guidelines for the care and use of laboratory animals. All animal experiments were conducted at Guangdong Huawei Testing Co., Ltd.

References

1. Jones IH, Hall NJ. Contemporary Outcomes for Infants with Necrotizing Enterocolitis-A Systematic Review. J Pediatr 2020;220:86-92.e3.
2. Duro D, Kalish LA, Johnston P, et al. Risk factors for intestinal failure in infants with necrotizing enterocolitis: a Glaser Pediatric Research Network study. J Pediatr 2010;157:203-208.e1.
3. Matei A, Montalva L, Goodbaum A, et al. Neurodevelopmental impairment in necrotising enterocolitis survivors: systematic review and meta-analysis. Arch Dis Child Fetal Neonatal Ed 2020;105:432-9.
4. Kaplina A, Kononova S, Zaikova E, et al. Necrotizing Enterocolitis: The Role of Hypoxia, Gut Microbiome, and Microbial Metabolites. Int J Mol Sci 2023;24:2471.
5. Hackam DJ, Sodhi CP. Bench to bedside - new insights into the pathogenesis of necrotizing enterocolitis. Nat Rev Gastroenterol Hepatol 2022;19:468-79.
6. Cheng H, Yu J, Dai L. A meta-analysis on the predictive role of CRP in NEC diagnosis and prognosis. Ital J Pediatr 2025;51:244.
7. Wu S, Ren X, Zhuang Y, et al. Peripheral Lymphocyte Changes Associate With the Progression of Necrotizing Enterocolitis in Infants. J Surg Res 2024;301:215-23.
8. Ng PC, Chan KYY, Yuen TP, et al. Plasma miR-1290 Is a Novel and Specific Biomarker for Early Diagnosis of Necrotizing Enterocolitis-Biomarker Discovery with Prospective Cohort Evaluation. J Pediatr 2019;205:83-90.e10.
9. Ng EW, Poon TC, Lam HS, et al. Gut-associated biomarkers L-FABP, I-FABP, and TFF3 and LIT score for diagnosis of surgical necrotizing enterocolitis in preterm infants. Ann Surg 2013;258:1111-8.
10. He S, Zhang XQ, Fu MR, et al. Diagnostic accuracy of gasdermin D as a biomarker for necrotizing enterocolitis: a single-center diagnostic test study. Transl Pediatr 2024;13:2134-43.
11. Li H, Lan C, Chen S, et al. Necrotizing enterocolitis: diagnosis with plasma IgG anti-tissue transglutaminase antibodies. Pediatr Res 2025;98:2278-83.
12. Davies MPA, Sato T, Ashoor H, et al. Plasma protein biomarkers for early prediction of lung cancer. EBioMedicine 2023;93:104686.
13. Ding P, Wu J, Wu H, et al. Transcriptomics-Based Liquid Biopsy for Early Detection of Recurrence in Locally Advanced Gastric Cancer. Adv Sci (Weinh) 2024;11:e2406276.
14. Tu Z, Bassal MA, Bell GW, et al. Tumor-suppressive activities for pogo transposable element derived with KRAB domain via ribosome biogenesis restriction. Mol Cell 2024;84:4209-4223.e6.
15. Mirabello L, Macari ER, Jessop L, et al. Whole-exome sequencing and functional studies identify RPS29 as a novel gene mutated in multicase Diamond-Blackfan anemia families. Blood 2014;124:24-32.
16. Xu W, Guo Z, Guan Y, et al. Machine learning-based proteomics profiling of ALS identifies downregulation of RPS29 that maintains protein homeostasis and STMN2 level. Commun Biol 2025;8:1177.
17. Jung YW, Shim JI, Shim SH, et al. Global gene expression analysis of cell-free RNA in amniotic fluid from women destined to develop preeclampsia. Medicine (Baltimore) 2019;98:e13971.
18. Walsh MC, Kliegman RM. Necrotizing enterocolitis: treatment based on staging criteria. Pediatr Clin North Am 1986;33:179-201.
19. Mu Y, Lan C, Chen J, et al. AQP-4 autoantibodies as potential early diagnostic biomarkers for NEC. Int Immunopharmacol 2025;159:114935.
20. Liu Y, Perego M, Xiao Q, et al. Lactoferrin-induced myeloid-derived suppressor cell therapy attenuates pathologic inflammatory conditions in newborn mice. J Clin Invest 2019;129:4261-75.
21. Zhou D, Yao M, Zhang L, et al. Adenosine Alleviates Necrotizing Enterocolitis by Enhancing the Immunosuppressive Function of Myeloid-Derived Suppressor Cells in Newborns. J Immunol 2022;209:401-11.

22. Rager TM, Olson JK, Zhou Y, et al. Exosomes secreted from bone marrow-derived mesenchymal stem cells protect the intestines from experimental necrotizing enterocolitis. J Pediatr Surg 2016;51:942-7.
23. Shi B, Shen L, Huang W, et al. A Nomogram for Predicting Surgical Timing in Neonates with Necrotizing Enterocolitis. J Clin Med 2023;12:3062.
24. Chen J, Zhong W, Hou L, et al. Predictive factors for rapid progression in preterm neonates with necrotizing enterocolitis. Front Pediatr 2022;10:970998.
25. Egan CE, Sodhi CP, Good M, et al. Toll-like receptor 4-mediated lymphocyte influx induces neonatal necrotizing enterocolitis. J Clin Invest 2016;126:495-508.
26. Lan C, Tian B, Shi Y, et al. CD177^{+} neutrophil-platelet aggregates contribute to thromboinflammation via NETs in necrotizing enterocolitis. Nat Commun 2026;17:4167.
27. Mohd Amin AT, Zaki RA, Friedmacher F, et al. C-reactive protein/albumin ratio is a prognostic indicator for predicting surgical intervention and mortality in neonates with necrotizing enterocolitis. Pediatr Surg Int 2021;37:881-6.
28. Zhang G, Wang X, Zhu S, et al. Hyponatremia as a Marker for Predicting Surgical Intervention in Necrotizing Enterocolitis: A Retrospective Cohort Study. J Surg Res 2024;295:364-9.
29. Chong Q, Wang Z, Guo T, et al. Gestational age-specific hematological features in preterm infants with necrotizing enterocolitis. Pediatr Res 2024;95:1826-36.
30. Cakir U, Tayman C, Yarci E, et al. Novel useful markers for follow-up of necrotizing enterocolitis: endocan and interleukin-33. J Matern Fetal Neonatal Med 2020;33:2333-41.
31. Ng PC, Chan KYY, Lam HS, et al. A Prospective Cohort Study of Fecal miR-223 and miR-451a as Noninvasive and Specific Biomarkers for Diagnosis of Necrotizing Enterocolitis in Preterm Infants. Neonatology 2020;117:555-61.
32. Tahmasebi S, Khoutorsky A, Mathews MB, et al. Translation deregulation in human disease. Nat Rev Mol Cell Biol 2018;19:791-807.
33. Lee JH, An CH, Kim MS, et al. Intratumoral Heterogeneity of RPL22 Frameshift Mutation in Colorectal Cancers. Pathol Oncol Res 2020;26:587-8.
34. Zhang Z, Wu Q, Fang M, et al. HERC3 directly targets RPL23A for ubiquitination degradation and further regulates Colorectal Cancer proliferation and the cell cycle. Int J Biol Sci 2022;18:3282-97.
35. de Almeida OP Jr, Toledo TR, Rossi D, et al. Hypusine modification of the ribosome-binding protein eIF5A, a target for new anti-inflammatory drugs: understanding the action of the inhibitor GC7 on a murine macrophage cell line. Curr Pharm Des 2014;20:284-92.
36. Figueiredo VC, Markworth JF, Durainayagam BR, et al. Impaired Ribosome Biogenesis and Skeletal Muscle Growth in a Murine Model of Inflammatory Bowel Disease. Inflamm Bowel Dis 2016;22:268-78.
37. Zhang J, Wang M, Yu D, et al. Transcriptome sequencing analysis identified an alternative splicing regulatory network mediated by RNA-binding proteins in asthma. J Asthma 2025;62:1798-806.
38. S Song S, Zhang D, Chen J, et al. CHMP4A stimulates CD8+ T-lymphocyte infiltration and inhibits breast tumor growth via the LSD1/IFNβ axis. Cancer Sci 2023;114:3162-75.
39. Lv W, Ma Y, Li D, et al. Single-Cell RNA Sequencing and Spatial Transcriptomics Reveal a Novel Mechanism of Oligodendrocyte-Neuron Interaction in Cognitive Decline After High-Altitude Cerebral Edema. CNS Neurosci Ther 2025;31:e70485.
40. Yu J, Hu S, Ma K, et al. Ribosomal protein S29 regulates metabolic insecticide resistance through binding and degradation of CYP6N3. PLoS One 2014;9:e94611.

Cite this article as: Wang Z, Zou P, Hou L, Lu J, Zeng J, Wei P, Ouyang Y, Tian Y, Zhong W, Lan C, Xia H, Song K. RPS29 as a potential early diagnostic biomarker for necrotizing enterocolitis: validation from transcriptomic and proteomic cohorts. Transl Pediatr 2026;15(5):176. doi: 10.21037/tp-2026-1-0077

